Available online at www.sciencedirect.com
SCIENCE DIRECT®

Journal of Organometallic Chemistry 691 (2006) 3003–3010

Journal of Organometallic Chemistry

www.elsevier.com/locate/jorganchem

Synthesis and structural studies of some titanium and zirconium complexes with chiral bis(amide), amidinate or bis(amidinate) ligands

JianFeng Li [a], ShuPing Huang [a], LinHong Weng [b], DianSheng Liu [a,*]

[a] *Modern Chemistry Institute, Shanxi University, Taiyuan, Shanxi 030006, China*
[b] *Department of Chemistry, Fudan University, Shanghai, China*

Received 8 October 2005; received in revised form 28 February 2006; accepted 7 March 2006
Available online 10 March 2006

Abstract

Reaction of bis(amide) sodium $Na_2[(1R,2R)\text{-}(-)\text{-}1,2\text{-}(NSiMe_3)_2\text{-}C_6H_{10}]$ ($Na_2[\mathbf{L}^1]$) with $Ti(OiPr)_2Cl_2$ in different conditions gave mixed-ligand complexes $[Ti(OiPr)Cl][\mathbf{L}^1]$ (**1**) or $[Ti(OiPr)_2Cl]_2[\mathbf{L}^1]$ (**2**); **2** is a dinuclear titanium example in which Ti atoms are bridged by nitrogen and oxygen atoms simultaneously forming a distorted rhombic core. Reaction of the amine-amidinate ligand $(1R,2R)\text{-}(-)\text{-}1\text{-}Li[NC(Ph)N(SiMe_3)]\text{-}2\text{-}(NHSiMe_3)\text{-}C_6H_{10}$ ($Li[\mathbf{L}^2]$) or rarely linked bis(amidinate) ligand $Li_2[(1R,2R)\text{-}(-)\text{-}1,2\text{-}\{NC(Ph)N(SiMe_3)\}_2\text{-}C_6H_{10}]$ ($Li_2[\mathbf{L}^3]$) with $ZrCl_4$ yielded the unbridged and bridged bis(amidinate) complexes $ZrCl_2[\mathbf{L}^2]_2$ (**3**) and $[ZrCl_2(THF)][\mathbf{L}^3]$ (**4**), respectively; Moreover, the reaction of $(1R,2R)\text{-}(-)\text{-}1\text{-}Li[NC(Ph)N(SiMe_3)]\text{-}2\text{-}Li(NSiMe_3)C_6H_{10}$ ($Li_2[\mathbf{L}^2]$) with $Ti(OiPr)_2Cl_2$ gave a new type of tridentate amido-amidinate product $[Ti(OiPr)_2][\mathbf{L}^2]$ (**6**), which is a distinct model compared to $[Ti(OiPr)_2Cl][\mathbf{L}^2]$ (**5**) yielded from $Li[\mathbf{L}^2]$. All the products have been characterized by X-ray crystallography and the structural studies are presented detailedly comparing with relevant compounds.

Keywords: Titanium; Zirconium; N ligands; Amidinate; Amide

1. Introduction

The Group 4 metal complexes containing bidentate N-donor ligands such as bis(amide), amidinate and β-diketiminate have drawn steady attention in recent years. The general type of bis(amide) complexes $(RN\text{-}L\text{-}NR)MX_2$ ($L =$ linking group) are promising systems for applications in catalysis because of their relationship to the well studied metallocene analogues Cp_2MX_2 [1], and bis(amide) $(R_2N)_2MX_2$ compounds [2]. Amidinates with three-atom bridging $NR'C(R'')NR^-$ framework have been proven to be versatile ligands due to the ease of presenting a flexible system of resultant metal compounds [3] with potential properties in homogeneous catalytic polymerization of a variety of hydrocarbon monomers including ethylene, propylene, 1,3-butadiene, and styrene [4]. The β-diketiminates have received significantly increased attention considering the scope for variation of the R groups on nitrogen and were investigated in our previous publications [5]. Both amidinates and β-diketiminates have delocalized π-electrons produced from various addition reactions of nitriles with anions [6].

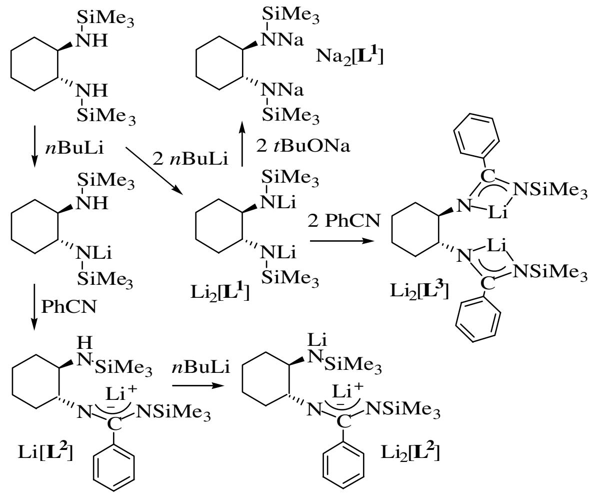

---

* Corresponding author. Fax: +86 351 7018091.
E-mail address: dsliu@sxu.edu.cn (D. Liu).

0022-328X/$ - see front matter © 2006 Elsevier B.V. All rights reserved.
doi:10.1016/j.jorganchem.2006.03.008

An attractive goal in bis(amide)- and amidinate-transition-metal chemistry consists in developing diversified ligation modes for exploitation of stereoselective catalysis using chiral ancillary ligands. Recently, we reported a series of useful chiral ligands derived from the well known scaffold (1*R*,2*R*)-1,2-diaminocyclohexane [7]. They are the chelated bis(amide) $Na_2[(1R,2R)\text{-}(-)\text{-}1,2\text{-}(NSiMe_3)_2\text{-}C_6H_{10}$ $(Na_2[\mathbf{L}^1])$ [8], the amine-amidinate $(1R,2R)\text{-}(-)\text{-}1\text{-}Li[NC(Ph)N(SiMe_3)]\text{-}2\text{-}(NHSiMe_3)\text{-}C_6H_{10}(Li[\mathbf{L}^2])$, the linked bis(amidinate) $Li_2[(1R,2R)\text{-}(-)\text{-}1,2\text{-}\{NC(Ph)N(SiMe_3)\}_2\text{-}C_6H_{10}](Li_2[\mathbf{L}^3])$ and a novel type of tridentate amido-amidinate ligation derived from $Li_2[\mathbf{L}^2]$ [9]. In related work, the *trans*-form of $\mathbf{L}^1$ has been reported to form titanium complexes [10]; the linked bis(amidinate) titanium [11] and yttrium [12] complexes show that the linking of two anionic ancillary moieties together by a covalent bridge results in an unusual ligand geometry. Herein, we present our further efforts to apply these ligands ($\mathbf{L}^1$, $\mathbf{L}^2$ and $\mathbf{L}^3$) in the synthesis of titanium and zirconium species including bis(amide) complexes $[Ti(OiPr)Cl][\mathbf{L}^1]$ (**1**) and $[Ti(OiPr)_2Cl]_2[\mathbf{L}^1]$ (**2**), unbridged and bridged bis(amidinate) complexes $[ZrCl_2][\mathbf{L}^2]_2$ (**3**) and $[ZrCl_2(THF)][\mathbf{L}^3]$ (**4**), amine-amidinate $[Ti(OiPr)_2Cl][\mathbf{L}^2]$ (**5**) and amido-amidinate $[Ti(OiPr)_2][\mathbf{L}^2]$ (**6**). Complex **2** is a noteworthy titanium example in which Ti atoms are bridged by both nitrogen and oxygen atoms [with Ti1···Ti2 distance as 3.204 Å]. The bridged zirconium complex of **4** with a chiral ancillary bis(amidinate) ligand shows different coordination behavior of the metal center comparing with the unbridged **3**. Titanium complexes **5** and **6** were previously communicated and their synthesis are discussed here [9a].

2. Results and discussion

2.1. Synthesis of 1–6

All these ligands, $\mathbf{L}^1$, $\mathbf{L}^2$ and $\mathbf{L}^3$, were systematically tried to the complexation with Group 4 metals. However, only **1**–**6** and $Zr[\mathbf{L}^1]_2$ were produced so far and the other attempt were unsuccessful (Scheme 1). For example, all the ligands, no matter lithium or sodium salts, mono- or di-anions, failed to give any products by the direct reaction with titanium tetrachlorides, although the reactions always yielded clear mother solution. Ti(IV) was presumed to be reduced by the reactant. This inspired us to modify the metal reagent to stable dicholorodialkoxides salt $Ti(OiPr)_2Cl_2$, and some interesting reactions were then revealed. All the effort applied to $HfCl_4$ failed too, no reaction phenomena happened in the solution after days stirring. For instance, $HfCl_4$ was finally recycled quantitatively from its reaction with $Na_2[\mathbf{L}^1]$ in toluene.

Certainly, ligands are synthesized and modified to behave different reactivities. As the immediate ligand, $Li_2[\mathbf{L}^1]$ was prepared by deprotonation of $(1R,2R)\text{-}(-)\text{-}1,2\text{-}(NHSiMe_3)_2\text{-}C_6H_{10}$ with 2 equiv. of *n*BuLi in hexane, however it shows very weak reactivity to all the metal reagents and no result was gained. The disodium salt $Na_2[\mathbf{L}^1]$, with intention to increase the reactivity, was thus synthesized as white precipitate by treatment of $Li_2[\mathbf{L}^1]$ with *t*BuONa in hexane. This method succeeded in three reactions (Scheme 1). The reaction of this bis(amide) ligand with $ZrCl_4$ in toluene gave bis-substituted tetradentate complex $Zr[\mathbf{L}^1]_2$ [8]. Its reaction with 1 equiv. of $Ti(OiPr)_2Cl_2$ in the donor solvent, THF, afforded $[(1R,2R)\text{-}(-)\text{-}1,2\text{-}(NSiMe_3)_2\text{-}C_6H_{10}][Ti(OiPr)Cl]$ (**1**). Interestingly, treatment of $Na_2[\mathbf{L}^1]$ with 2 equiv. of $Ti(OiPr)_2Cl_2$ in the nonpolar solvent, hexane, resulted in a dinuclear complex $[(1R,2R)\text{-}(-)\text{-}1,2\text{-}(NSiMe_3)_2\text{-}C_6H_{10}][Ti(OiPr)_2Cl]_2$ (**2**), showing the diversified results of this versatile metal reagent and ligand in different reaction conditions.

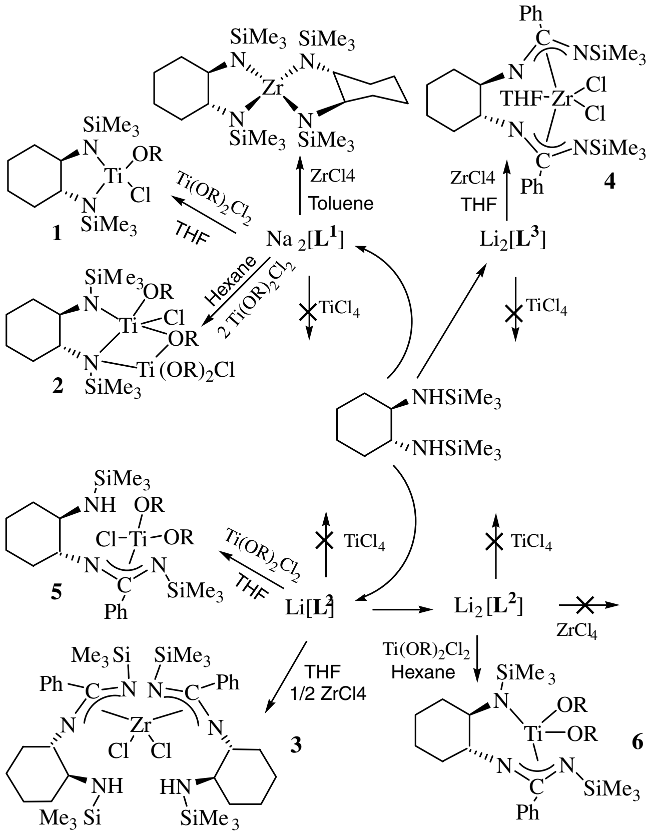

Scheme 1. Synthesis of the **1**–**6** and related reactions (R = *i*Pr).

Treatment of monolithium ligand $(1R,2R)\text{-}(-)\text{-}1\text{-}Li(NSiMe_3)\text{-}2\text{-}(NHSiMe_3)\text{-}C_6H_{10}$ $(Li[\mathbf{L}^1])$ with 1 equiv. of benzonitrile gave the amine-amidinate $(1R,2R)\text{-}(-)\text{-}1\text{-}Li[NC(Ph)N(SiMe_3)]\text{-}2\text{-}(NHSiMe_3)\text{-}C_6H_{10}(Li[\mathbf{L}^2])$. This type of addition reaction of an anionic amine with nitrile was firstly reported by Sanger [13]. Monoanionic $Li[\mathbf{L}^2]$ was initially treated with one equivalent of $ZrCl_4$ in THF and once assumed to give a three-coordinate product. Unexpectually, the reaction afforded 2:1 ratio product $[(1R,2R)\text{-}(-)\text{-}1\text{-}[NC(Ph)N(SiMe_3)]\text{-}2\text{-}(NHSiMe_3)\text{-}C_6H_{10}]_2\text{-}ZrCl_2$ (**3**). **3** is an unbridged bis(amidinate) zirconium complex, where the pendant amine groups dissociate and this differs from our prediction and some relevant work, in which a lone pair of electrons of pendant amine groups coordinates to the central metals forming a tridentate coordinated environment [14]. Similarly, when reacted with Ti(O*i*Pr)$_2$Cl$_2$ in THF, Li[**L**^{2}] gave amidinate complex of [(1*R*,2*R*)-(−)-1-{NC(Ph)N(SiMe$_3$)}-2-{N(H)SiMe$_3$C$_6$H$_{10}$]-[Ti(OiPr)$_2$Cl] (**5**) in didentate model with the pendant amine group dissociates from the central metal as that in **3**.

These molecular structure results arose our interest to develop new coordination model. Li$_2$[**L**^{2}] was thus synthesized by further deprotonation of Li[**L**^{2}] with 1 equiv. of *n*BuLi in hexane. We anticipated that this dianionic amido-amidinate ligand Li[**L**^{2}] will produce a new type of tridentate fashion where the amidinate fragment bonded to the central metal with η^3–π bond, and at the same time the pendant amide group forming a σ bond, compared to the lone pair of electrons of pendant amine groups coordinated to the central metals [14]. The reaction of Li$_2$[**L**^{2}] with Ti(O*i*Pr)$_2$Cl$_2$ in hexane yielded a new complex of [(1*R*,2*R*)-(−)-1-{NC(Ph)N(SiMe$_3$)}-2-(NSiMe$_3$)C$_6$H$_{10}$][Ti-(O*i*Pr)$_2$] (**6**) [9a]. The structural characterization of **6** confirmed our hypothesis of new tridentate framework, which is a distinct comparison to the simple didentate amidinate-liganded complex **5** [9a]. Unfortunately, our hard effort to produce similar zirconium complex failed.

Treatment of dilithium ligand Li$_2$[**L**^{1}] with 2 equiv. of benzonitrile generated double-addition reaction and gave linked bis(amidinate) ligand Li$_2$[**L**^{3}]. The reaction of Li$_2$[**L**^{3}] with ZrCl$_4$ in THF followed by extraction with dichloromethane gave the corresponding zirconium complex [(1*R*,2*R*)-(−)-1,2-{NC(Ph)N(SiMe$_3$)}$_2$-C$_6$H$_{10}$]ZrCl$_2$-(THF) (**4**) (Scheme 1) in 78% isolated yield. The presence of a coordinated molecule of THF in **4** causes some difference in molecular structure from the unbridged bis(amidinate) zirconium complex **3** and analogue [C$_6$H$_5$C(NSiMe$_3$)$_2$]$_2$ZrCl$_2$ (**9**) [15].

2.2. NMR spectroscopy

For the titanium complexes, ^{1}H NMR spectra showed characteristic resonance for the protons of cyclohexane groups in the regions of δ 1.23–1.77 (**1**) and 1.33–1.81 (**2**). The SiMe$_3$ groups in **1** showed single resonance, however in **2** they appeared as two separate peaks (δ 0.15 and 0.17) because of the different coordinated environment. Two kinds of methyl protons were found in **2**, δ 0.29 (2×3H) for the isopropoxy group bridging the two metal atoms and δ 1.29 (6×3H) for the remaining isopropoxy groups. In ^{13}C NMR spectra, **1** showed carbon resonances of cyclohexane as three peaks at δ 26.22, 27.99, 35.62 and the methine carbon of the isopropoxy group at δ 76.36; while four methine carbon peaks were detected at δ 64.75, 72.81, 79.69 and 80.72 for the isopropoxy groups in **2**.

The zirconium complex **3** showed its four SiMe$_3$ groups as two separate single peaks at δ −0.07 and −0.02 suggesting its symmetric structure in solution. For complex **4** the characteristic resonances for the protons of cyclohexane group appeared in the regions of δ 0.83–3.04 and THF at δ 1.90 (2×2H), 3.95 (2×2H). Additional support for the identification of the products is provided by the ^{13}C NMR spectra. Two kinds of tertiary carbons in amidinate fragments were found at δ 135.30, 183.55 for **3** and 138.06, 179.72 for **4**, respectively.

2.3. Crystal structures of complexes 1–4

The molecular structure of **1** is shown in Fig. 1 and selected bond distances and angles are listed in Table 1. All the amide nitrogens are sp^2-hybridized (sum of angles around $N1 = 358.3°$, $N2 = 360.0°$). The cyclohexane ring adopts a chair conformation with the two SiMe$_3$ groups in equatorial position, and the C–C–N–Ti–N ring adopts an envelop conformation. The geometry around Ti is distorted tetrahedral with the N–Ti–N angle as 92.1(2)°.

The molecular structure of **2** is illustrated in Fig. 2 and selected bond distances and angles are listed in Table 2. In this dinuclear molecule, the cyclohexane makes a rigid bicyclic core with the five-membered N1–Ti1–N2–C6–C1 ring. Different from **1**, the two SiMe$_3$ groups are in unsymmetric positions with one distorted strongly allowing for the coordination of the other Ti(O*i*Pr)$_2$Cl group. N1 is three-co-ordinate and N2 four-co-ordinate and bridging.

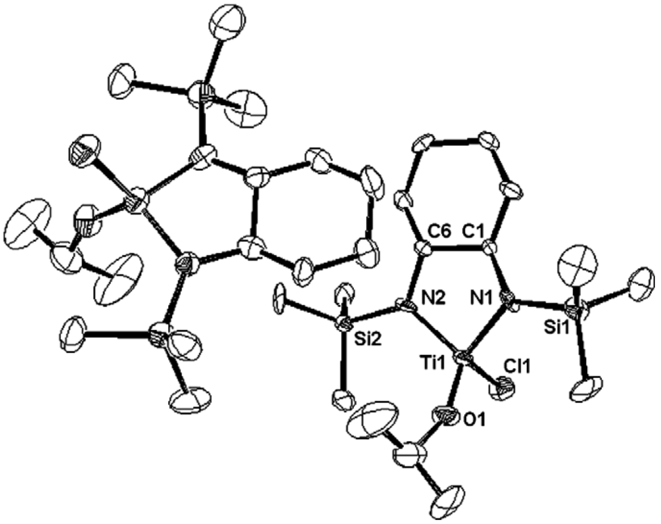

Fig. 1. ORTEP view of **1** with thermal ellipsoids at 50% probability level, all hydrogen omitted for clarity.

Table 1
Selected bond distances (Å) and angles (°) for **1**

Ti1–N1	1.879(5)	Ti1–N2	1.876(5)
Ti1–O1	1.763(4)	Ti1–Cl1	2.288(2)
N1–C1	1.497(7)	N2–C6	1.477(7)
N1–Ti1–N2	92.1(2)	O1–Ti1–Cl1	112.80(17)
C1–N1–Si1	126.5(4)	Cl1–Ti1–N1	110.13(17)
Si2–N2–Ti1	124.2(3)	C6–N2–Si2	127.3(4)
C6–N2–Ti1	108.5(4)	C1–N1–Ti1	103.8(3)

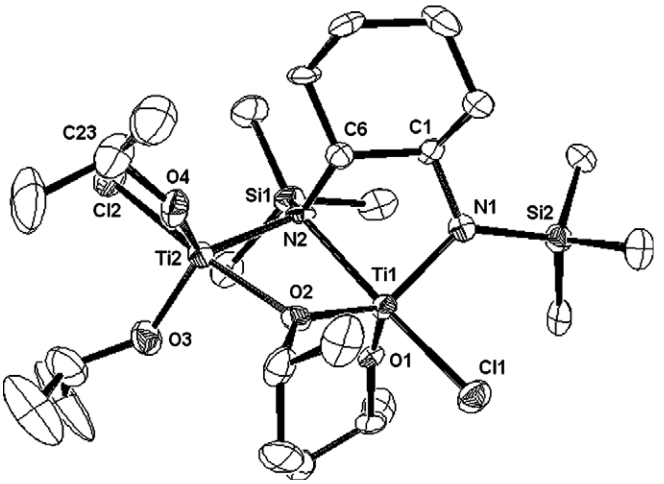

Fig. 2. ORTEP view of **2** with thermal ellipsoids at 50% probability level, all hydrogen omitted for clarity.

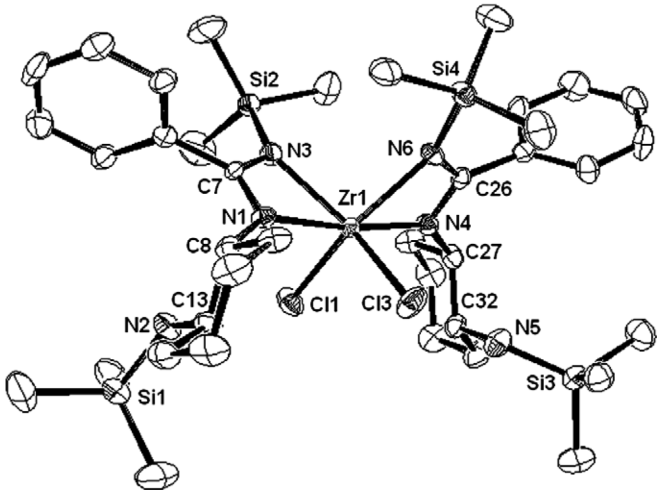

Fig. 3. ORTEP view of **3** with thermal ellipsoids at 40% probability level, all hydrogen omitted for clarity.

Table 2
Selected bond distances (Å) and angles (°) for **2**

Ti1–N1	1.907(5)	Ti1–N2	2.196(5)
Ti1–O1	1.734(5)	Ti2–N2	2.070(5)
Ti1–O2	1.968(4)	Ti2–O2	2.020(4)
Ti2–O3	1.766(5)	N2–C6	1.466(8)
Ti2–N2–Ti1	97.4(2)	Ti1–O2–Ti2	106.9(2)
O2–Ti1–N2	74.50(19)	O2–Ti2–N2	76.30(19)
C6–N2–Ti2	106.4(4)	C6–N2–Ti1	96.6(4)
N1–Ti1–N2	82.6(2)	C1–N1–Ti1	113.9(4)
C1–N1–Si2	119.7(4)	C6–N2–Si1	119.9(4)

Table 3
Selected bond distances (Å) and angles (°) for **3**

C8–N1	1.481(6)	C7–N1	1.315(5)
C1–C7	1.492(7)	N3–C7	1.350(6)
N3–Zr1	2.184(3)	N1–Zr1	2.239(4)
C7–Zr1	2.641(5)	N4–C26	1.324(6)
C26–Zr1	2.645(5)	N6–Zr1	2.206(4)
N1–C7–N3	113.4(4)	C7–N1–Zr1	92.2(3)
Cl1–Zr1–Cl3	101.44(6)	N1–Zr1–N4	172.74(14)
N3–Zr1–N6	91.76(15)	N3–Zr1–N1	60.46(14)
C7–N3–Zr1	93.7(3)	N4–Zr1–N6	60.50(16)

Unexpectedly, O2 bonds to Ti2 and bridges both titanium atoms with similar bond distances [Ti1–O2 1.968(4) and Ti2–O2 2.020(4) Å], and these values are considerably larger than terminal σ bonds of Ti1–O1 [1.734(5) Å] and Ti2–O3 [1.766(5) Å]. The two bridging atoms and the metal atoms build up a four-membered distorted plane N2–Ti1–O2–Ti2 (with dihedral angle between Ti1–O2–Ti2 and Ti1–N2–Ti2 as 26.7°). Although their tetherings are different, the two Ti atoms [with Ti1···Ti2 distance as 3.204 Å] are both five–co-ordinated.

The molecular structure of **3** is showed in Fig. 3 and selected bond distances and angles are listed in Table 3. It is noticed that the two pendant amine groups are far apart from the metal center (≈4.1 Å) and thus show a unbridged bis(amidinate) coordinate model. The two cyclohexane rings adopt the chair conformation and the central zirconium atom is coordinated in a distorted tetrahedral fashion by two benzamidinate ligands and two chlorine atoms. The two N–C–N fragments (as η^3-anion having some degree of π-electron delocalisation) are bonded to the central zirconium atom forming two four-membered rings. The dihedral angle between these two mean planes (N1–C7–N3–Zr1 and N4–C26–N6–Zr1) is 80.9°; meanwhile, the dihedral angles between each of them and the phenyl rings they attached to are 97.0° and 96.8°, respectively.

The molecular structure of **4** is illustrated in Fig. 4 and selected bond distances and angles are listed in Table 4. The whole molecule takes an approximately latitudinal coordinate model with a linear three-atom Cl2–Zr1–O1 [angle 179.90(13)°] axis. The two benzamidinate moieties form two near coplanar N–Zr–N–C rings [e.g., torsion angle of N2–Zr1–N3–C7 = −8.0(3)°], while the dihedral

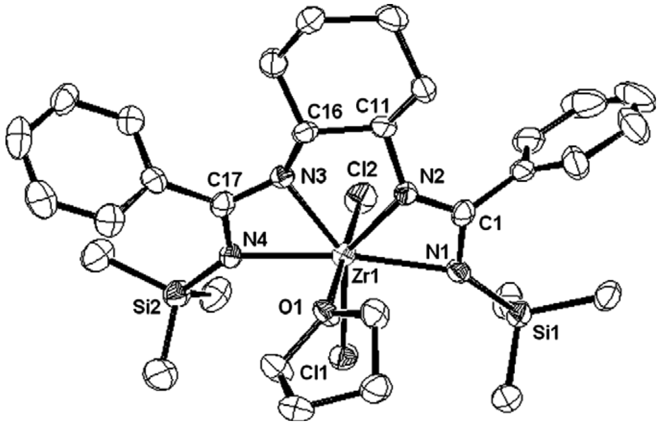

Fig. 4. ORTEP view of **4** with thermal ellipsoids at 50% probability level, all hydrogen omitted for clarity.

Table 4
Selected bond distances (Å) and angles (°) for **4**

Zr1–N1	2.169(5)	Zr1–N2	2.183(4)
Zr1–N3	2.285(4)	Zr1–N4	2.319(4)
Zr1–O1	2.260(4)	Zr1–C7	2.688(5)
Zr1–C14	2.606(5)	Zr1–Cl1	2.5032(17)
N2–C7	1.333(6)	N3–C7	1.346(7)
N2–Zr1–N3	59.06(17)	N1–Zr1–N4	59.02(16)
N1–Zr1–N2	69.25(17)	N3–Zr1–N4	171.04(15)
C7–Zr1–C14	127.01(19)	N2–C7–N3	110.7(5)
N2–C2–C1	103.8(4)	N1–C1–C2	104.0(4)
Cl2–Zr1–Cl1	94.38(6)	O1–Zr1–Cl2	179.90(13)

angle between these two mean planes is only 6.7°, totally different from that of **3** (80.9°) and confirming the latitudinal model in whole molecule. It is also found that there is a considerable difference between Zr–N distances for terminal nitrogen atoms and those linked to the cyclohexane; for example, Zr1–N2 [2.183(4) Å] is shorter than Zr1–N4 [2.319(4) Å].

Comparison of structural data for the related chelated bis(amide) titanium compounds [{(±)-*trans*-1,2-$(NSiMe_3)_2$-C_6H_{10}}$Ti(CH_2Ph)_2$] (**7**) and [{(±)-*trans*-1,2-$(NSiMe_3)_2$-C_6H_{10}}TiI_2] (**8**) [10] with data for **1** and **2** reveals some noteworthy features. Key bond angles and distances for the selected compounds are listed in Table 5. In compound **2**, the N(2)–Ti bond is longer than the N(1)–Ti bond, and they are both longer than those in **1**, **7** and **8**. In the comparison of the five-membered C(1)–C(2)–N(2)–Ti–N(1) ring, N(1)–Ti–N(2), O–Ti–Cl and C(2)–N(2)–Ti angles of **2** decreases by 9–10°, 18°, and 12°, while the C(1)–N(1)–Ti angle increases by 6–10° relative to the corresponding values in **1**, **7** and **8**. The C(1)–N(1)–Si angle of **2** is also restricted somewhat because of the distorted $SiMe_3$ group. These different geometric features obviously result from the additional co-ordination of the second Ti–$(OiPr)_2$Cl group in compound **2**. In addition, the Ti coordination number in **2** is five because of the bridging oxygen atom.

The study on the key bonds and angles of **3**, **4** and the unbridged bis(amidinate) complex $[C_6H_5C(NSiMe_3)_2]_2ZrCl_2$ (**9**) gives further comprehension of their ligand geometry (Table 6). All the N–C–N fragments of these three complexes have π-electron delocalisation present as η^3-anions and explain their relatively short C(Ph)–N distances. The bond lengths of Zr–N(1) and Zr–N(2) in **3** and **7** are similar (all around 2.21 ± 0.03 Å), but in **4** there is some difference in the Zr–N distances for the amidinate nitrogen attached to the cyclohexyl [2.169(5) Å] compared to that attached to the $SiMe_3$ group [2.319(4) Å]. In compound **4**, the two nitrogen atoms on cyclohexane bond to the zirconium atom forming a five-membered ring and thus give a rigid bicyclic core with the cyclohexane. This geometry therefore restricts the angle of C(2)–C(1)–N(1) [104.0(4)°] and the torsion angle of N–C(2)–C(1)–N(1) [44.3(6)°], both of which reflect the *trans* character of the diaminocyclohexane. This geometry as well as restricts the dihedral angle between the two N–Zr–N–C(Ph) mean planes in **4** [only 6.7 compared to 80.9° (**3**) and 79.9° (**9**)] giving a expanded sphere which allows coordination space for an additional molecule of THF and consequently results in a reduction of Cl–Zr–Cl angle [94.38(6)° compared to 101.44(6)° (**3**) and 103.78(5)° (**9**)]. In addition, the two dihedral angles between N–Zr–N–C(Ph) and phenyl rings (96.3° and 58.6°) in **4** are much different compared with that in **3** (96.8° and 97.0°). They are, however, still large enough to inhibit an effective conjugation between the two π-systems of phenyl ring and amidinate group.

Table 5
Some selected geometric data (bond lengths in Å, angles in°) on **1**, **2**, **7** (x = CH_2Ph) and **8** (x = I) ; (R = $SiMe_3$; R′ = *i*Pr)

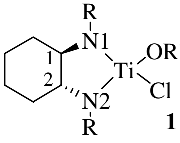

1

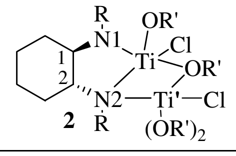

2

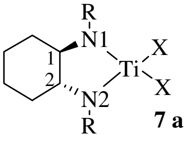

7 and 8

	1	2	7	8
N(1)–Ti	1.879(5)	1.907(5)	1.879(1)	1.836(2)
N(2)–Ti	1.876(5)	2.196(5)	–	–
N(1)–Ti–N(2)	92.1(2)	82.6(2)	91.97(8)	93.0(2)
C(1)–N(1)–Ti	103.8(3)	113.9(4)	107.73(9)	107.9(2)
C(2)–N(2)–Ti	108.5(4)	96.6(4)	–	–
C(1)–N(1)–Si	126.5(4)	119.7(4)	124.9(1)	123.7(2)
O–Ti–Cl	112.80(17)	94.37(17)	–	–
Co-ordination number at Ti	4	5	4	4

Table 6
Some selected geometric data (bond lengths in Å, angles in °) on **3**, **4** and **9** (R = $SiMe_3$)

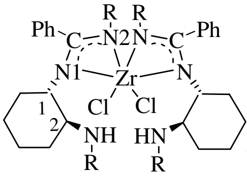

3

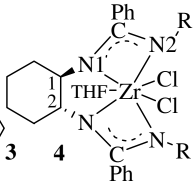

4

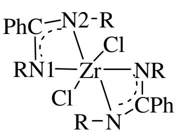

9

	3	4	9
C(Ph)–N(1)	1.315(5)	1.340(6)	1.320(3)
C(Ph)–N(2)	1.350(6)	1.324(7)	1.337(3)
Zr–N(1)	2.239(4)	2.169(5)	2.240(2)
Zr–N(2)	2.184(3)	2.319(4)	2.201(2)
Cl–Zr–Cl	101.44(6)	94.38(6)	103.78(5)
C(2)–C(1)–N(1)	110.4(4)	104.0(4)	–
N(1)–C(1)–C(2)–N	56.7	44.3	–
α[a]	80.9	6.7	79.9
β[b]	96.8	96.3	74.3
	97.0	58.6	–

[a] Dihedral angles between the two N–Zr–N–C(Ph) mean planes.

[b] Dihedral angles between N–Zr–N–C(Ph) mean plane and the attached phenyl ring.

3. Experimental

3.1. General remarks

All manipulations were carried out under argon, using standard high-vacuum, Schlenk techniques. Deuterated solvents C_6D_6, $CDCl_3$ were dried over activated molecular sieves (3 Å) and vacuum transferred before use. Hexane, Et_2O, THF were distilled from Na or Na/K alloy before use, except for chlorinated solvents which were distilled from activated molecular sieves (3 Å) or CaH_2. Benzonitrile was redistilled and dried over activated molecular sieves (4 Å) before use. The compounds Na_2[**L**^{1}], Li[**L**^{2}] and Li_2[**L**^{3}] were prepared according to the literature procedures. ^{1}H(300 MHz) and ^{13}C (75.47 MHz) NMR spectra were recorded on a Bruker DRX-300 spectrometer at ambient temperature. Element analysis were performed by Analysis Center of Shanxi University.

3.2. Preparations

3.2.1. *[(1R, 2R)-(−)-1,2-(NSiMe$_3$)$_2$-C$_6$H$_{10}$][Ti(OiPr)Cl] (**1**)*

To a solution of Na_2[**L**^{1}] (0.345 g, 1.14 mmol) in 25 mL of THF was added Ti(O*i*Pr)$_2$Cl$_2$ (0.27 g, 1.14 mmol) at −78 °C. The mixture was warmed to room temperature slowly, and stirred overnight. The solvent was removed in vacuum and the residual solid was extracted with hexane (20 mL). The extract was concentrated to ca. 10 mL and cooled to −10 °C yielded 0.23 g (51%) of **1**. $C_{15}H_{35}ClN_2OSi_2Ti$ (398.98): Anal. Calc. C, 45.15; H, 8.84; N, 7.02. Found: C, 45.48; H, 8.79; N, 7.23%. ^{1}H NMR ($CDCl_3$): $\delta = 0.18$ (s, 9H, SiMe$_3$), 1.23 (m, 4H, CH), 1.33 (m, 6H, OCHC$_2$*H*$_6$), 1.45 (m, 4H, CH), 1.77 (m, 2H, CH), 4.67 (m, 1H, OC*H*C$_2$H$_6$). ^{13}C NMR ($CDCl_3$): $\delta = 2.75$ (SiMe$_3$), 26.22 (NCC*C*), 27.49 (OC*C*), 27.64 (OC*C*), 27.99 (NC*C*), 35.62 (N*C*), 68.85 (O*C*C).

3.2.2. *[(1R,2R)-(−)-1,2-(NSiMe$_3$)$_2$-C$_6$H$_{10}$][Ti(OiPr)$_2$Cl]$_2$ (**2**)*

To a solution of Na_2[**L**^{1}] (0.55 g, 1.82 mmol) in 35 mL of hexane was added Ti(O*i*Pr)$_2$Cl$_2$ (0.862 g, 3.64 mmol) at 0 °C. The mixture was warmed to room temperature and stirred overnight. Subsequently, the solvent was filtered and reduced to ca. 10 mL. Cooling to −20 °C for 2 days and yielded 0.96 g (80%) of crystalline **2**. $C_{24}H_{56}C_{12}N_2O_4Si_2Ti_2$ (659.59): Anal. Calc. C, 43.70; H, 8.56; N, 4.25. Found: C, 43.91; H, 8.50; N, 4.14%. ^{1}H NMR ($CDCl_3$): $\delta = 0.15$ (s, 9H, SiMe$_3$), 0.17 (s, 9H, SiMe$_3$), 1.29–1.33 (d, 24H, OCHC$_2$*H*$_6$), 1.33–1.81 (m, 6H, C$_6$*H*$_6$), 4.35 (m, 1H, OC*H*C$_2$H$_6$), 4.64 (m, 1H, OC*H*C$_2$H$_6$), 4.72 (m, 1H, OC*H*C$_2$H$_6$), 4.86 (m, 1H, OC*H*C$_2$H$_6$). ^{13}C NMR ($CDCl_3$): δ 1.63 (SiMe$_3$), 2.20 (SiMe$_3$), 25.32 (NCC*C*), 25.95 (OC*C*), 26.51 (OC*C*), 27.07(OC*C*), 33.91(NC*C*), 34.86 (N*C*), 64.75 (O*C*C), 72.81 (O*C*C), 79.69 (O*C*C), 80.72 (O*C*C).

3.2.3. *[(1R,2R)-(−)-1-[NC(Ph)N(SiMe$_3$)]-2-(NHSiMe$_3$)-C$_6$H$_{10}$]$_2$ZrCl$_2$ (**3**)*

To a solution of Li[**L**^{2}] (0.46 g, 1.25 mmol) in 30 mL of THF was added $ZrCl_4$ (0.146 g, 0.63 mmol) at −78 °C. The mixture was warmed to room temperature slowly, stirred for 12 h. Subsequently, the solvent was removed in vacuum and the residual solid was extracted with CH_2Cl_2 (15 mL). The extract was concentrated to ca. 5 mL and cooled to −10 °C yielded 0.44 g (80%) of crystalline **3**. $C_{38}H_{66}Cl_2N_6Si_4Zr$ (881.45): Anal. Calc. C, 51.92; H, 7.57; N, 9.57. Found: C, 51.51; H, 7.68; N, 9.38%. ^{1}H NMR ($CDCl_3$): $\delta = -0.07$ (s, 9H, NSiMe$_3$), −0.02 (s, 9H, NSiMe$_3$), 0.97 (m, 2H, CH), 1.39 (m, 2H, CH), 1.67 (m, 4H, CH), 1.98 (m, 1H, CH), 2.81 (m, 1H, CH), 7.33 (m, 2H, Ph), 7.42 (m, 3H, Ph). ^{13}C NMR ($CDCl_3$): $\delta = 1.83$ (SiMe$_3$), 2.86 (SiMe$_3$), 25.77 (NCC*C*), 26.04 (NCC*C*), 33.98 (NC*C*), 55.99 (CN), 67.37 (CN), 126.07–130.01 (*C*$_5$H$_5$), 135.30 (*C*C$_5$H$_5$), 183.55 (*C*Ph).

3.2.4. *[(1R,2R)-(−)-1,2-{NC(Ph)N(SiMe$_3$)}$_2$-C$_6$H$_{10}$]ZrCl$_2$(THF) (**4**)*

To a solution of Li_2[**L**^{3}] (0.715 g, 1.50 mmol) in 35 mL of THF was added $ZrCl_4$ (3.51 g, 1.51 mmol) at −78 °C. The mixture was warmed to room temperature slowly, stirred for 12 h. Subsequently, the solvent was removed in vacuum and the residual solid was extracted with CH_2Cl_2 (20 mL). The extract was concentrated to ca. 10 mL and cooled to −10 °C yielded 0.82 g (78%) of crystalline **4**. $C_{30}H_{46}C_{12}N_4OSi_2Zr$ (697.01): Anal. Calc. C, 51.69; H, 6.65; N, 8.04. Found: C, 50.92; H, 6.80; N, 7.90%. ^{1}H NMR ($CDCl_3$): $\delta = -0.05$ (s, 18H, SiMe$_3$), 0.83 (m, 2H, CH), 1.21 (m, 2H, CH), 1.38 (m, 2H, CH), 1.54 (m, 2H, CH), 1.90 (m, 4H, CH THF), 3.04 (m, 2H, CH), 3.95 (m, 4H, CH THF), 7.36 (m, 10H, Ph). ^{13}C NMR ($CDCl_3$): $\delta = 2.82$ (SiMe$_3$), 25.20 (NCC*C*), 26.08 (OC*C*), 34.29 (NC*C*), 67.88 (N*C*), 71.43 (O*C*), 127.53–130.67 (*C*$_5$H$_5$), 138.06 (*C*C$_5$H$_5$), 179.72 (*C*Ph).

3.2.5. *[(1R,2R)-(−)-1-{NC(Ph)N(SiMe$_3$)}-2-{N(H)SiMe$_3$}C$_6$H$_{10}$][Ti(OiPr)$_2$Cl] (**5**)*

Ref. [9a].

3.2.6. *[(1R, 2R)-(−)-1-{NC(Ph)N(SiMe$_3$)}-2-(NSiMe$_3$)C$_6$H$_{10}$][Ti(OiPr)$_2$] (**6**)*

Ref. [9a].

3.3. X-ray crystallographic study

Pertinent details for individual compounds can be found in Table 7. A crystal of appropriate size was mounted using inert handling techniques into the cold nitrogen stream of an Bruker SMART APEX diffractometer/CCD area detector utilizing graphite-monochromatized Mo Kα radiation ($\lambda = 0.71073$ Å). A hemisphere of data was collected, and the raw data were then integrated (*XY* spot spread = 1.60°; *Z* spot spread = 0.60°) (SAINT) [16]. A total of *N* reflections were collected by using ω scan mode. Corrections were

Table 7
Crystallographic data for **1**–**4**

	1	**2**	**3**	**4**
Empirical formula	$C_{15}H_{35}ClN_2OSi_2Ti$	$C_{24}H_{56}Cl_2N_2O_4Si_2Ti_2$	$C_{38}H_{66}Cl_2N_6Si_4Zr$	$C_{30}H_{46}Cl_2N_4OSi_2Zr$
Formula mass	398.98	659.59	881.45	697.01
Temperature (K)	180(2)	183(2)	173(2)	174(2)
Wavelength (Å)	0.71073	0.71073	0.71073	0.71073
Crystal system	Monoclinic	Monoclinic	Monoclinic	Orthorhombic
Space group	$P2_1$	C_2	$P2_1$	$P2_12_12_1$
a (Å)	10.472(2)	16.3649(17)	10.316(2)	8.0810(18)
b (Å)	10.077(2)	10.5364(12)	16.219(4)	10.383(2)
c (Å)	21.269(4)	20.584(2)	14.638(3)	41.738(9)
α (°)	90.00	90.00	90.00	90.00
β (°)	96.74(3)	98.779(2)	96.566(3)	90.00
γ (°)	90.00	90.00	90.00	90.00
Volume ($Å^3$)	2228.9(8)	3507.6(7)	2433.2(9)	3502.1(13)
Z	4	4	2	4
Crystal size (mm)	0.40 × 0.40 × 0.20	0.20 × 0.20 × 0.10	0.40 × 0.40 × 0.30	0.20 × 0.20 × 0.10
Absorption coefficient (mm^{-1})	0.614	0.704	0.465	0.563
Reflections collected	10917	6237	10550	15808
Goodness-of-fit on F^2	1.105	1.050	1.008	1.018
Independent reflections	6605	5471	7138	6815
R_{int}	0.0427	0.0396	0.0474	0.0648
Final R indices [$I > 2\sigma(I)$]	$R_1 = 0.0746$	$R_1 = 0.0734$	$R_1 = 0.0556$	$R_1 = 0.0689$
	$wR_2 = 0.1337$	$wR_2 = 0.1113$	$wR_2 = 0.0788$	$wR_2 = 0.1006$
R (all data)	$R_1 = 0.0934$	$R_1 = 0.0848$	$R_1 = 0.0680$	$R_1 = 0.0887$
	$wR_2 = 0.1432$	$wR_2 = 0.1162$	$wR_2 = 0.0821$	$wR_2 = 0.1065$
Largest different peak/hole (e $Å^{-3}$)	0.58/−0.43	0.54/−0.41	0.87/−0.58	1.13/−0.61

applied for Lorentz and polarization effects as well as absorption using multi-scans (SADABS) [17]. The structure was solved by direct method (SHELXS-97) [18]. Then the remaining non-hydrogen atoms were obtained from the successive difference fourier map. All non-H atoms were refined with anisotropic displacement parameters, while the H atoms were constrained to parent sites, using a riding model (SHELXTL) [19].

Acknowledgement

We thank the Natural Science Foundation of China (20472046, D.-S. Liu).

Appendix A. Supplementary data

Crystallographic data for the structural analysis have been deposited with the Cambridge Crystallographic Data Center, CCDC Nos. 183018, 183017, 183019, 173962, 183020 and 191954 for complexes **1**, **2**, **3**, **4**, **5** and **6**, respectively. Supplementary data associated with this article can be found, in the online version, at doi:10.1016/j.jorganchem.2006.03.008.

References

[1] (a) D.J. Cardin, M.F. Lappert, C.L. Raston, Chemistry of Organo-Zirconium and -Hafnium Compounds, Halsted Press, New York, 1986;
(b) H.H. Brintzinger, D. Fischer, R. Mulhaupt, B. Rieger, R.M. Waymouth, Angew. Chem., Int. Ed. Engl. 34 (1995) 1143–1170.

[2] (a) R.K. Minhas, L. Scoles, S. Wong, S. Gambarotta, Organometallics 15 (1996) 1113–1121;
(b) C.H. Lee, Y.-H. La, J.W. Park, Organometallics 19 (2000) 344–351;
(c) N.A.H. Male, M. Thornton-Pett, M. Bochmann, J. Chem. Soc., Dalton Trans. (1997) 2487–2494.

[3] (a) F.T. Edelmann, Coord. Chem. Rev. 137 (1994) 403–481;
(b) J. Barker, M. Kilner, Coord. Chem. Rev. 133 (1994) 219–300;
(c) Martyn P. Coles, Dale C. Swenson, Richard F. Jordan, Organometallics 16 (1997) 5183–5194.

[4] (a) J.C. Flores, J.C.W. Chien, M.D. Rausch, Organometallics 14 (1995) 1827–1833;
(b) A. Littke, N. Sleiman, C. Bensimon, D.S. Richeson, Organometallics 17 (1998) 446–451;
(c) V. Volkis, M. Shmulinson, C. Averbuj, Organometallics 17 (1998) 3155–3157.

[5] (a) Peter B. Hitchcock, Michael F. Lappert, Marcus Layh, Dian-Sheng Liu, Rafael Sablong, Tian Shun, J. Chem. Soc., Dalton Trans. (2000) 2301–2312;
(b) Laurence Bourget-Merle, Michael F. Lappert, John R. Severn, Chem. Rev. 102 (2002) 3031–3066;
(c) Peter B. Hitchcock, Michael F. Lappert, D.-S. Liu, J. Chem. Soc., Chem. Commun. (1994) 1699–1700.

[6] (a) Scott E. Schaus, Jonas Branalt, Eric N. Jacobsen, J. Org. Chem. 63 (1998) 403–405;
(b) Barry M. Trost, Michael J. Krische, Rumen Radinov, Giuseppe Zanoni, J. Am. Chem. Soc. 118 (1996) 6297–6298.

[7] Jian-Feng Li, Lin-Hong Weng, Xue-Hong Wei, Dian-Sheng Liu, J. Chem. Soc., Dalton Trans. 07 (2002) 1401–1405.

[8] Jian-Feng Li, Lin-Hong Weng, Shu-Ping Huang, Hong-Bo Tong, Dian-Sheng Liu, Acta Crystallogr., Sect. E 58 (2002) m510–m512.

[9] (a) Jian-Feng Li, Shu-Ping Huang, Lin-Hong Weng, Dian-Sheng Liu, Eur. J. Inorg. Chem. (2003) 810–813;
(b) Jian-Feng Li, Lin-Hong Weng, Shu-Ping Huang, Hong-Bo Tong, Dian-Sheng Liu, Acta Crystallogr., Sect. E 58 (2002) o1078–o1080.

[10] Barbara Tsuie, Dale C. Swenson, Richard F. Jordan, Jeffrey L. Peterson, Organometallics 16 (1997) 1392–1400.

[11] (a) John R. Hagadorn, John Arnold, Angew. Chem., Int. Ed. Engl. 37 (1998) 1729–1731;
(b) Glenn D. Whitener, John R. Hagadorn, John Arnold, J. Chem. Soc., Dalton Trans. (1999) 1249–1256.

[12] Sergio Bambirra, Auke Meetsma, Bart Hessen, Jan H. Teuben, Organometallics 20 (2001) 782–785.

[13] A.R. Sanger, Inorg. Nucl. Chem. Lett. 9 (1973) 351–354.

[14] D. Doyle, Y.K. Gun Ko, P.B. Hitchcock, M.F. Lappert, J. Chem. Soc., Dalton Trans. (2002) 4093–4097.

[15] (a) Dorit Herskovics-Korine, Moris S. Eisen, J. Organomet. Chem. 503 (1995) 307–314;
(b) Unpublished work and the data presented here refers to our work.

[16] SAINT: SAX Area-Detector Integration Program, Madison, WI, 1995.

[17] G.M. Sheldrick, Correction Software, University of Göttingen, Germany, 1996.

[18] G.M. Sheldrick, Program for the Solution of Crystal Structures, University of Göttingen, Germany, 1997.

[19] Program for Crystal Structure Refinement, Bruker Analytical X-ray Instruments Inc., Madison, WI, USA, 1998.